Journal of
Plankton Research

academic.oup.com/plankt

J. Plankton Res. (2021) 43(6): 831–845. First published online October 23, 2021 https://doi.org/10.1093/plankt/fbab071

ORIGINAL ARTICLE

Protoplasmic streaming of chloroplasts enables rapid photoacclimation in large diatoms

VLADIMIR SILKIN[1], ALEXEY FEDOROV[1], KEVIN J. FLYNN[2,*], LEONID PARAMONOV[1] AND LARISA PAUTOVA[1]

[1]SHIRSHOV INSTITUTE OF OCEANOLOGY, RUSSIAN ACADEMY OF SCIENCES, MOSCOW 117997, RUSSIA AND [2]PLYMOUTH MARINE LABORATORY, PROSPECT PLACE, PLYMOUTH PL1 3DH, UK

*CORRESPONDING AUTHOR: kjf@pml.ac.uk

Received April 23, 2021; revised September 7, 2021; accepted September 24, 2021

Corresponding editor: Lisa Campbell

Long-term (2004–2020) studies showed yearly summer/autumn blooms in the NE Black Sea dominated by large (cell volume > 5000 μm^3) diatoms (*Pseudosolenia calcar-avis* and *Proboscia alata*). This phenomenon is characterized by high (>250 W m^{-2} photosynthetically active radiation, PAR) insolation, and low phosphorus concentrations (to analytical zero). These diatoms contained >100 chloroplasts per cell, which at low irradiance are evenly distributed throughout the cell. As light increases (to 1000 μmol photons m^{-2} s^{-1} PAR), chloroplasts aggregate within 20 min, usually to the center of the cell. In consequence, the light absorption coefficient is decreased by >3 fold. At elevated photon flux density (PFD), *P. calcar-avis* also shows a "conveyor" of chloroplasts moving from the aggregate to the cell periphery and back. This mechanism enables a continuous fine-tuning of the cells' ability to absorb light, likely also facilitating photo-damage repair. This rapid photoacclimation mechanism allows large diatoms to minimize photodamage at high PFD and acclimate well to low PFD. We hypothesize that competitive success of large diatoms in conditions of high light gradients is aided by this short-term rapid photoacclimation enhancing growth rate while minimizing chloroplast repair costs, aided by the ability of large cells to accumulate nutrients for chloroplast synthesis.

KEYWORDS: phytoplankton; large diatoms; allometry; chloroplast; photoacclimation; succession; *P. calcar-avis*

available online at academic.oup.com/plankt

INTRODUCTION

Diatoms are one of the most successful taxonomic groups of phytoplankton, support a highly productive part of the ocean's pelagic ecosystem, and play a key role in the silicon cycle's functioning (Smetacek, 1999; Armbrust 2009; Treguer and De La Rocha, 2013). This taxonomic group is represented by a wide size spectrum of cells and has the characteristic feature of forming a cell shell made of silica. The shell architecture creates a robust structure that is resistant to mechanical damage, grazers, and virus penetration (Hamm *et al*., 2003).

Large-cell forms play an essential role in the ocean ecosystem from the equator to polar latitudes (Goldman, 1993; Kemp *et al*., 2006; Villareal *et al*., 1996; Villareal *et al*., 2012). The significance of large cells could be viewed as surprising because large celled-organisms are often considered poor competitors for nutrients due to biophysical size-related constraints (Chisholm, 1992). The kinetic parameters of nutrient uptake by large diatoms (Edwards *et al*., 2012) suggest that under stable conditions, the evolution of a mixed population should always lead to the displacement of large diatoms and that small cells will dominate. However, diatoms also have a relatively low density of C per cell volume (gC L^{-1} cell volume) which becomes increasingly important at higher cells sizes (Menden-Deuer and Lessard, 2000), lowering the physiological cell surface-area:volume ratio penalty for nutrient transport (Flynn *et al*., 2018). There are also other hypotheses that have been used to help explain large diatoms' dominance, which can be divided into two classes—biotic and abiotic.

Of the biotic factors, a major regulator of phytoplankton community size structure is top-down grazing pressure (Kiørboe 2008, 2011; Ward *et al*., 2012). Large diatom cells are an inconvenient food due to their size for the more abundant microzooplankton (Wirtz, 2012); the predator takes out the smaller species and, thus, the size phytoplankton structure is regulated by the grazers (Wirtz and Sommer, 2013). For those that graze on these large diatoms, their lowered gC: cell-volume also makes them a lower-value food package than similarly sized other plankton (McBeain and Halsey, 2018). In addition, a new hypothesis proposes that a niche for large diatoms exists because of the non-static dynamics of the predator–prey ratio (Behrenfeld *et al*., 2021a, 2021b); the existence of some lag time before the appearance of an adequate-sized predator allows large diatoms to grow intensively. It is also likely that large-celled phytoplankton are relatively less susceptible to virus attack because although larger cells are more likely to encounter viruses, the decreased cell abundance provides insufficient hosts to support high rates of virus attack (Flynn *et al*., 2021).

Hypotheses centered on an abiotic regulation of phytoplankton structure imply that large cells can only be successful in a dynamic environment (Margalef, 1978; Villamaña *et al*., 2019). In the modern interpretation of the Margalef mandala, one of the coordinates is duration and magnitude of change in limiting resources (Behrenfeld *et al*., 2021b). Thus, with weak changes in limiting resources, small diatoms are suggested to gain the advantage; large diatoms are more successful with significant environmental change. The heterogeneity of the environment over time allows for dominance of species with different sizes in the population (Huisman *et al*., 2006). Periodic wind mixing supports the introduction of nutrients into the upper mixed layer (UML), which may be taken up and accumulated in large diatoms (Raven, 1987; Flynn *et al*., 2018) and are then used in growth processes. This mechanism is based on the so-called storage hypothesis (Tozzi *et al*., 2004; Verdy *et al*., 2009), and mathematical modeling shows the potential ability for such a mechanism to ensure the dominance of large cells (Grover, 1989, 1997; Stolte and Riegman, 1996; Abakumov *et al*., 2011). However, recently this hypothesis has been brought into question (Behrenfeld *et al*., 2021a).

Nutrient transport limitations for large cells may also be mitigated by fine-scale turbulence (Barton *et al*., 2014) and, for diatoms, by the aforementioned advantage in having a low gC:cell volume ratio (Flynn *et al*., 2018). In addition, cells of large diatoms are able to regulate their buoyancy, enabling them to move into waters with higher nutrient concentrations to enhance nutrient uptake rates (Villareal *et al*., 1996; Gemmell *et al*., 2016). However, all this emphasis on top-down control and nutrient acquisition ignores the essential role of photosynthesis as a determining factor in success; what of the ability of large diatoms to maximize their photosynthetic rate relative to that of smaller diatoms?

Net photosynthesis is a function of gross photosynthesis versus expenditure on synthesis and maintenance of all cellular components, including chloroplasts. Long-term photoacclimation is distinguished by, and it is associated with, changes in the cellular concentration of chlorophyll (Falkowski and Owens, 1980; Richardson *et al*., 1983; Falkowski and LaRoche, 1991; MacIntyre *et al*., 2002). Short-term photoacclimation is associated with the formation of a photo-protective pigments cycle (Raven and Geider, 2003; Raven, 2011). However, diatoms growing in the high light gradient of a dynamic UML, with its deep thermocline, are constantly subjected to rapid changes in the conflicting pressures of photoacclimation vs photo-inhibition/damage repair in response to the changing light flux and spectral composition. The required response time to maintain efficiency in such an

environment ranges from minutes to hours. In this context, the photoenergetic aspect of large cells' dominance is associated with their ability to resist photoinhibition due to the package effect (Duysens, 1956; Finkel, 2001; Finkel and Irwin, 2000; Key *et al*., 2010; Kirk, 2011). This effect occurs through the formation of layers of chloroplasts which in a large cell results in internal self-shading. This event has the potential to prevent photodamage of the light-harvesting pigment complex and, as a result, the need to expend energy and resources on repair (Raven, 2011).

A chaotic environment is supportive of the coexistence of cells of different sizes. The fluctuating light regime generates different effects on the community's structure and is one of the factors enabling the coexistence of species (Litchman and Klausmeier, 2001). While the storage hypothesis may allow species of different size to coexist, it cannot explain phenomena in nature when, for a long time, the diatom component is represented by a single species of large diatoms. Thus, long-term observations in the NE part of the Black Sea have shown that every year in the summer season, one species of *P. calcar-avis* dominates; its contribution to the total phytoplankton biomass exceeds 90%. At the same time, other diatoms' existence is excluded (Silkin *et al*., 2019). An understanding of the mechanisms underlying the absolute dominance of large diatoms is needed. This is of fundamental importance since the transition from the dominance of small-cell phytoplankton to the predominance of large diatoms affects the structure of the food chain and, as a result, the biogeochemical functions of the ocean ecosystem (Laws *et al*., 2000).

In this paper we propose a hypothesis that helps to explain the exceptional competitive success of *P. calcar-avis*, which can be extended to other species of large diatoms. We hypothesize that the rapid redistribution of chloroplasts within the cell in response to changing irradiance provides these large diatoms with a significant advantage, notably enhancing photosynthesis at low light but critically also minimizing cell destruction due to photodamage of chloroplasts. An appreciation of a role for the redistribution of chloroplasts within cells as a mitigation strategy against photoinhibition developed many decades ago, termed systrophe by Jenkin (1937). Such movements of chloroplasts and the resulting heterogeneity of their distribution in the cell when irradiance changes (Kiefer, 1973; Blatt *et al*., 1981; Chen and Li, 1991; Furukawa *et al*., 1998; Goessling *et al*., 2016) is of fundamental importance in the formation of the optical properties of the cell (Richardson *et al*., 1996) and, as a result, determines the photoenergetic capacity of the cell (Stephens, 1995). The mechanism provides a means for a rapid response to changes in photon fluxes, as a form of short-term acclimation that is more rapid than may be achieved through synthesis and breakdown of chloroplasts.

Fig. 1. Map of the research area in the Black Sea in 2004–2020.

To explore our hypothesis, we investigated the phenomenon of large-cell diatom blooms, determined the physical and chemical environments of their dominance, studied the shape of chloroplasts and their composition inside the cell with changes in irradiance, detected movement of chloroplasts by a protoplasmic conveyor system, and calculated the optical properties of single chloroplasts and in a chloroplast aggregates.

METHOD

Field sampling

Hydrophysical, hydrochemical, and phytoplankton composition data were obtained on numerous cruise of different R/V from 2004 to 2020. The study area covered the entire NE part of the Black Sea (Fig. 1). A CTD (Sea-Bird Electronics, Inc.) was used to measure temperature, salinity, and density, and thence to estimate the UML depth.

Water samples for nutrient concentrations and phytoplankton composition were collected using 5 L Niskin bottles mounted on a Rosette sampler. At each station, samples were taken from the surface, the middle of the upper mixed layer, the seasonal thermocline, and below the thermocline. Phytoplankton samples (bottles of 1–1.5 L) were fixed with neutralized formaldehyde (0.8–1.0% final concentration). Samples were processed within one month; the milder fixation used better preserved the plankton over this period. Samples were stored in darkness, at room temperature (ca. 18–20°C), for two weeks; after cell sedimentation, the upper water layers were slowly decanted.

Field sample analyses

Concentrations of silicate, phosphate (P), nitrate (NO_3^-), nitrite (NO_2^-), and ammonium (NH_4^+) were obtained using standard spectrophotometric techniques (Bordovskiy and Chernyakova, 1992; Grashoff *et al*., 1999), with the same frequency as phytoplankton sampling. Total dissolved inorganic nitrogen (DIN) was estimated as nitrate, nitrite, and ammonium. Over the entire study period, 1700 samples for these nutrients were collected.

Plankton were analyzed by light microscopy (Jenaval, Carl Zeiss "Jena") with 16 × 20 and 16 × 40 magnifications used for species identification and cell counting. Cells with linear dimensions of less than 20 μm were counted with a Naujotte chamber (0.05 mL). Counts were considered sufficient when at least 100 cells of each species were counted. A Naumann (1 mL) chamber was used to count larger cells. Usually, an entire Naumann's chamber was counted. When calculating phytoplankton total biomass, cells with linear dimensions of less than 2 μm were not considered.

Species identification was based on morphology, according to Tomas (1997) and Throndsen *et al*., (2003), and the World Register of Marine Species (http://www.marinespecies.org). Cells with unknown taxonomic affiliation of 4 to 10 μm were classified as "small flagellates". Cell volume was estimated according to Hillebrand *et al*. (1999). For each sample, the biomass of each species was calculated; total biomass was as the sum of the biomass of all species. Conversion from biovolume to carbon biomass units was carried out using equations (Menden-Deuer and Lessard, 2000). The dominant species was considered as that whose biomass accounted for more than half of the total biomass of phytoplankton at this station. The subdominant species was the second most abundant species by biomass. The total number of phytoplankton samples used in our study was 1700. Wet weight was computed from the cell biovolume assuming cell density is equal to 1 g mL^{-1}.

Experimental studies

The study of chloroplasts' movement and the formation of plastid aggregates were performed at the coastal laboratory of the Southern Branch of the P.P. Shirshov Institute of Oceanology (Gelendzhik) both with natural samples and after their maintenance in culture under different light conditions. Water was sampled in 5-L bottles with simultaneous filtration through two layers of the net (mesh size—30 μm) to remove smaller plankton. The remaining large cells on the mesh net were studied immediately or transferred to a 0.5-L Erlenmeyer flask. These flasks were kept in a chamber where the temperature and illumination were regulated. Water temperature was usually maintained at the same value of the sea surface at the time of sampling. Lighting was supplied using LEDs (SMD 5050, cold white light, 6500 K), and the photon flux density (PFD) varied from 0 to 350 μmol photons m^{-2} s^{-1} PAR; the light:dark cycle was 16:8.

Studies on the effects of light on the movement of chloroplasts were carried out under a light microscope (Jenaval, Carl Zeiss "Jena") at a magnification from 16 × 10 to 16 × 40. The effects of irradiance on chloroplast movement were studied when PFD was changed. To do this, cells from a natural population or from a culture were viewed by microscope and the location of the chloroplasts was recorded at low irradiance (ca. 20–35 μmol quanta m^{-2} s^{-1} PAR). Next, the irradiance was increased to values of 500, 800, or 1000 μmol quanta m^{-2} s^{-1} PAR, the cells held at that continuous irradiance and the distribution and movement of the chloroplasts recorded by camera (Nikon D5200, Nikon corporation). Quantitative assessment was carried out using the obtained images. The speed of movement and turnover time of chloroplasts in the cell were measured from visual analysis of video films.

Estimates of absorption coefficients

The specific absorption coefficient of chlorophyll *in vivo* and chlorophyll concentration in the cell is used to evaluate the cell's optical properties. For a laboratory monoculture, this procedure can be done with simple measurements. The specific absorption coefficient of chlorophyll *in vivo* can be obtained by measuring an algae suspension's absorption spectrum on an integrating sphere spectrophotometer. Standard methods can calculate the concentration of chlorophyll. However, this approach is not applicable to the natural population. In the present study we estimated the absorbed energy of the chloroplast and the cell.

A light microscope was used to estimate the number of chloroplasts in living cells, their aggregation, and shape. In contrast to the chlorophyll concentration distribution in the cell, which is very variable and difficult to determine, the chlorophyll content in chloroplasts (β_{Chl}) may be assumed to be constant with a value of 30 moles m^{-3} (Nobel, 2005) or 26 mg mL^{-1}. The chloroplast volume is equated to a geometric shape, an ellipsoid or cylinder, and the chloroplast volume then calculated using this shape's formula. The length of the light path, l, is calculated accordingly:

$$\text{For cylinder} : l = \frac{2\,r\,h}{r+h}$$

where r is the radius and h is the height of cylinder.

$$\text{For ellipsoid : } l = \frac{2a\ b\ c}{2a + \frac{b\ c}{2}}$$

where is the a and b is the semi-minor axis and c is the semi-major axis.

Aggregates are assumed to be cylindrical. The average length of the light path $<l>$ is then calculated for these geometric shapes.

When estimating the volume absorption coefficient of diatoms chloroplast $a_V(\lambda)$ ($\mu m^{-1} = \mu m^2 \cdot \mu m^{-3}$), which characterizes the absorption by a unit of chloroplast volume, we used the following ratio (Paramonov, 2018):

$$a_V(\lambda) = \frac{1 - e^{-a^*(\lambda)\cdot\beta_{Chl}\cdot<l>}}{<l>} \quad (1)$$

where λ is the wavelength (nm).

We used the spectrum of specific absorption coefficients of pigments solution $a^*(\lambda)$ of the centric diatom *Chaetoceros protuberans* (Hoepffner and Sathyendranath, 1991). These specific absorption spectra were reconstructed (Paramonov, 2018) (Table S1).

The average-specific absorption coefficient was calculated using Eq. (2).

$$a_V = \frac{\int_{400}^{700} a_V(\lambda)\, d\lambda}{\int_{400}^{700} d\lambda} \quad (2)$$

Statistical methods

Comparison between two samples were made using a *t*-test, with a significance level of $P < 0.05$.

RESULTS

Main dominant large diatoms and subdominants of the north-eastern part of the Black Sea

Long-term observations (2004–2020) of the Black Sea phytoplankton structure revealed the main dominant large diatoms (Table I). In the summer, usually from the beginning of July, large-celled diatoms dominated. Most cells were of *P. calcar-avis* (40 000 μm^3 cell volume), with a maximum biomass level of 4700 mg wet weight m^{-3} (137.2 mg Cm^{-3}) seen in July 2014; the maximum contribution by this species to the total phytoplankton biomass (excluding picoplankton) was 97.2%. Sometimes

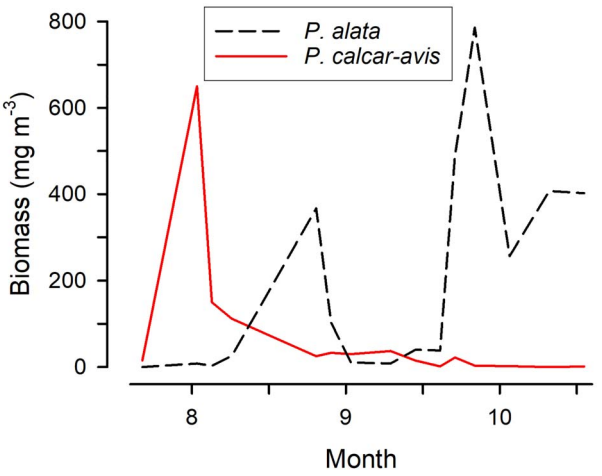

Fig. 2. Dynamics of the surface water biomass, as wet weight, of the diatoms *P. calcar-avis* (ca. 40 000 μm^3 cell volume) and *P. alata* (ca. 20 000 μm^3 cell volume) in the coastal water near Geledgzhik (Fig. 1) in July–October 2015.

in the summer months, the dominant diatom was *P. alata* (20 000 μm^3 cell volume), whose biomass reached 4000 mg wet weight m^{-3} (122.0 mg C m^{-3}) (June 2009), and the contribution to the total biomass >93%. In 2015, we observed a more complex series of dynamics for diatom abundance in coastal waters, in which the usual summer dominant *P. calcar-avis* with biomass above 600 mg wet weight m^{-3} in early August was replaced by another large diatom, *P. alata*, which in turn had its own complex dynamics (Fig. 2).

In September, there was a change of dominance; the primary phytoplankton species was now the large-cell diatom *P. alata*; the maximum level of biomass of more than 3600 mg wet weight m^{-3} (112.8 mg C m^{-3}) was recorded in October 2009, the contribution to the total biomass being 99%. In some years, the summer dominant *P. calcar-avis* maintained its dominance into September, and its biomass attained 1917 mg wet weight m^{-3} (56.9 mg C m^{-3}) in September 2011, with the maximum contribution to the total biomass > 90.3%. In November 2011, an alternative dominant diatom, *Hemiaulus hauckii*, with a relatively low biomass level, periodically appeared in the phytoplankton.

Physico-chemical conditions for the dominance of large diatoms

The Black Sea does not freeze; in winter, the water temperature rarely falls below 7.0°C. The maximum temperature during our survey years was recorded in August, at 28.03°C (August 25, 2013, shelf). In summer and autumn, when large diatoms dominated, the water temperature

Table I: Dominant phytoplankton species, their maximal biomass and share in the total biomass in the NE part of the Black Sea in the period from 2004 to 2020. Data are given for the UML

Season	Species and average cell volume	Date	Maximal biomass, mg wet weight m^{-3}	Share in the total biomass, %
Summer	*P. calcar-avis*	July 2014	4718	97.2
	P. alata	June 2009	4016	93.0
Autumn	*P. alata*	October 2009	3667	97.0
	P. calcar-avis	September 2011	1917	90.3
	H. hauckii	November 2011	154	56.0

was 25.7 ± 0.2 and 21.2 ± 0.3°C (Fig. S1 in Supplementary Material). The average long-term temperature in August, when *P. calcar-avis* blooms, was 26.4°C.

In summer, high insolation levels were recorded in the north-eastern part of the sea, with virtually no clouds (Fig. S2 in Supplementary Material). During *P. calcar-avis* blooms, in July and August, the irradiation was 262 ± 4.1 and 230 ± 3.9 $W \cdot m^{-2}$, respectively. Changes in salinity during the summer period were insignificant, with salinity being 17.77 ± 0.19.

A characteristic feature of the hydrophysical conditions of large diatoms' dominance was the deepening of the seasonal thermocline (Fig. S3 in Supplementary Material). In early June, the thermocline was closest to the water surface (ca. 10 m); from the second half of June, the permanent deepening of the seasonal thermocline began. During the *P. calcar-avis* blooms, the thermocline was mainly located at a depth of 20–30 m.

Size, quantity, morphology, and distribution of diatom chloroplasts

The chloroplasts of diatoms had different sizes and have a different share of the total cell volume. The diatoms of interest here, which are dominant phytoplankton of the Black Sea, included small pennate diatoms (for example, *Pseudo-nitzschia pseudodelicatissima* and *Thalassionema nitzschioides*) and also the large centric diatoms *P. calcar-avis, P. alata*, and *H. hauckii* (Table II). The former usually had two chloroplasts (*P. delicatissima*) or more (*T. nitzschioides*) (Fig. S4 in Supplementary Material). The latter had a large number of chloroplasts; in *P. calcar-avis*, their number reached 150 chloroplasts per cell.

Reaction of the diatoms to changes in PFD

Large species of centric diatoms had a completely different response to increased irradiance to those seen in smaller species. Thus, the increased PFD induced the movement of chloroplasts in *Dactyliosolen fragilissimus* and the formation of chloroplast aggregates near the wall (Fig. S5, in Supplementary Material), the time for formation of these aggregates was 10–20 min. In the diatom *Cerataulina pelagica*, when the PFD increases, the chloroplasts also began to move and form from one to three aggregates per cell (Fig. S6, in Supplementary Material).

The large centric diatoms *P. calcar-avis* and *P. alata* also displayed different chloroplast movement patterns depending on the PFD. In low PFD, the chloroplasts were distributed evenly throughout the cell (Fig. 3a), and at high PFD, a chloroplast aggregate was formed, located in the cell's center (Figs 3b and S7, in Supplementary Material). In the cells of *P. calcar-avis* and *H. hauckii*, the formation of an aggregate was also accompanied by continuous chloroplast movements along the cell wall, forming a kind of conveyor that connected the aggregate and the cell periphery (Figs 3b and S7 in Supplementary Material). This is shown in a schematic in Fig. 4, and in a video clip in Supplementary Media. The cycle duration of a chloroplast through such a conveyor was 5–15 minutes, depending on the species and PFD. The chloroplasts of *H. hauckii* traveled a shorter path due to the morphological features of the cell (Fig. S7, in Supplementary Material); they moved at a slower conveyor speed compared to *P. calcar-avis* in the autumn samples. However, the time of such rearrangements of the chloroplast was always less than 20 minutes, and, therefore, they can be classified as short-term acclimation.

On average, about 30% of the chloroplasts were in the conveyor, and the remaining 70% remained in the aggregate. Assuming that all chloroplasts were handled in the same way, the average time spent by the chloroplast in the aggregate varied from 20 to 50 minutes. Also, we noted a rotation of chloroplasts within aggregates; chloroplasts move from the cell wall to the center of the aggregate and back. A more prolonged exposure to bright light resulted in a loss of the ability to move and form an aggregate of chloroplasts.

Photoenergetic properties of large diatoms

The specific rate of cell growth μ (day^{-1}) depends on the amount of absorbed light energy (PAR) per unit of

Table II: Morphophysiological parameters of phytoplankton dominants: h and d—cell length and diameter, μm; V_{cell}- cell volume, μm³; V_{Chlst}—chloroplast volume, μm³; <l> — average light path length, μm

Species	h	d	V_{cell}	V_{Chlst}	<l>
S. costatum	10	5	196	28.3	2.25
Pseudo-nitzschizia spp.	70	3	330	62.8	1.88
Leptocylindrus danicus	60	5	1178	8.4	1.60
C. affinis	15	10	1178	125.6	2.79
C. curvisetus	20	15	3533	251.2	2.89
C. pelagica	70	12	7913	18.8	1.33
D. fragilissimus	80	15	14 130	18.8	1.60
P. alata	500	7	19 233	7.1	1.33
H. hauckii	80	20	25 120	20.9	1.43
P. calcar-avis	500	10	39 250	9.4	1.29

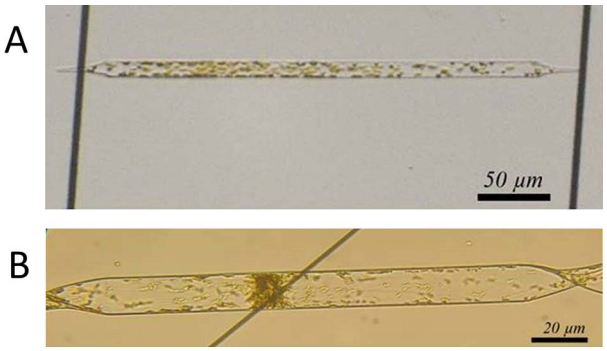

Fig. 3. Panel (**a**) shows the uniform distribution of chloroplasts inside cell of a large diatom *P. alata* at low PFD (near 20 μmol photons m^{-2} s^{-1} PAR). In this case, the increased PFD set the chloroplasts in motion and the formation of the aggregate begins. Panel (**b**) shows the formation of the chloroplast aggregate and conveyor of chloroplasts in large diatoms *P. calcar-avis* with increasing PFD up to 500 μmol photons m^{-2} s^{-1} PAR. About 30% of the chloroplasts are in the conveyor belt and move clockwise along the cell wall. The remaining 70% are located in the aggregate where there is a continuous movement from the center of the cell to the walls and back.

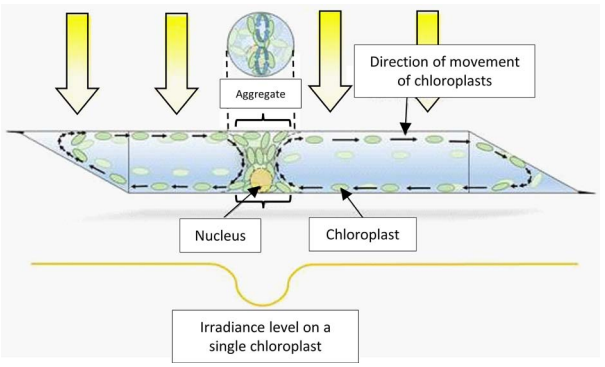

Fig. 4. Schematic showing the formation of the chloroplast aggregate and conveyor and rotation of chloroplasts within the aggregate in large diatoms with increasing PFD. Chloroplasts are shown viewed at different angles and focal depths to the viewer, hence their different color shades. See also the video in Supplementary Media.

biomass or volume Q_J (W·(g dry weight)$^{-1}$ or W m^{-3}) and the efficiency of its use in growth processes Υ_I (g dry weight W^{-1}) and the rate of dark respiration μ_o (day^{-1}) (Droop *et al*., 1982):

$$\mu = \Upsilon_I \, Q_J - \mu_o = \Upsilon_I \, \frac{I_{absorb}}{W_S} - \mu_o = \varphi \, k \, \frac{I_{absorb}}{W_S} - \mu_o \quad (3)$$

Here, W_S is cell biomass per unit area of the illuminated surface (g dry weight m^{-2}), I_{absorb} is absorbed light energy (W·(g dry weight)$^{-1}$), φ is the quantum yield of growth (dimensionless), and k is the conversion coefficient from biomass units to energy units (g dry weight Joule^{-1}).

The absorbed energy is determined by the specific absorption coefficient of the cellular substance, which depends on the pigments' composition with a characteristic absorption spectrum for each and the content of pigments in the cell (Kirk, 2011). The *in vivo* absorption spectrum differs significantly from the absorption spectrum of the solution of these pigments; the morphological organization of the cellular structure determines this. The ratio of the *in vivo* absorption spectrum to the absorption spectrum of the solution of these pigments is called the Q_ϱ package effect (Morel and Bricaud, 1981), with a value always less than 1. For phytoplankton cells growing in the UML, the irradiance varies from the maximum at the water surface to the minimum at the seasonal thermocline's depth. If we consider the average illumination for this water column, I_{av}, we can rewrite Eq. (3) as:

$$\mu = \varphi \, k \, \varrho \, I_{av} \, a_{Chl} \frac{\beta_{Chl}}{W_{cell}} - \mu_o \quad (4)$$

where I_{av} is as per Eq. (5).

$$I_{av} = I_0 \frac{1 - e^{-z_t k_d}}{z_t k_d} \quad (5)$$

Here, W_{cell} is cell biomass (g dry weight cell^{-1}), I_{av} is the average irradiance (Wm^{-2}), a_{Chl} is the chlorophyll-specific light absorption coefficient (m^2 (g chl)$^{-1}$), β_{Chl} is

chlorophyll content in the cell (g chl cell^{-1}), ϱ is the ratio of daylight hours to 24 hours (dimensionless), k_d is the light attenuation coefficient (m^{-1}), z_t is the depth of the UML (m), and I_0 is the surface irradiance (W m^{-2}).

In general, parameters a_{Chl}, β_{Chl}, φ, and W_{cell} are light-dependent functions. Thus, the specific absorption coefficient of chlorophyll a_{Chl} increases with a significant increase PFD (Geider *et al*., 1998; Suggett *et al*., 2007), while the efficiency of light energy use φ (Sydko *et al*., 1966; Kiefer and Mitchell, 1983) and the content of chlorophyll in the cell both decrease (Richardson *et al*., 1983; Geider *et al*., 1986; Falkowski and LaRoche, 1991; MacIntyre *et al*., 2002; Finkel *et al*., 2004). The carbon content in the cell increases as PFD increases (MacIntyre *et al*., 2002).

Assuming a constant pigment concentration in the phytoplankton cell, significant variations in volume-based absorption coefficients are possible. Such variations are due to the package effects of the pigments in the cells, of which there are two types:

1) the absorption coefficients depending on the size and shape of the cells; these are determined by the average length of the light path that passed through the cell—this is the package effect of the first kind (Duysens, 1956);
2) the absorption coefficient depending on the distribution of pigments inside the cells and the peculiarities of the formation of the chloroplast aggregates—this is the package effect of the second kind.

The first kind of package effect on various marine phytoplankton species has been considered by many researchers (Agusti, 1991; Finkel and Irwin, 2000; Finkel, 2001). Figure 5 shows calculated specific absorption coefficients per unit cell volume $a_V(\lambda)$ for the dominant phytoplankton species in our survey, with a dispersed distribution of chloroplasts in the cell and the identical concentration chlorophyll in the cell. It takes into account the package effect of the first kind. It follows from Fig. 5 that the absorbed energy quite clearly separated two groups of diatoms. The first group included *P. pseudodelicatissima, Skeletonema costatum, T. nitzschioides*. These species shared one property—they had a small cell volume (up to 1000 μm^3). The remaining diatoms had a cell volume above 5000 μm^3. The calculated volume-specific absorption coefficients of these groups differed significantly with $P < 0.01$ (Table S2).

The second kind of package effect is a function of the formation of aggregates of chloroplasts, through which large diatoms can realize short-term acclimation. This packaging gives the cell completely different optical properties. This kind of short-term acclimation leads to a decrease in the chlorophyll-specific absorption coefficient, which must be quantified. To do this, it is necessary to know the morphometric characteristics of cells and chloroplasts.

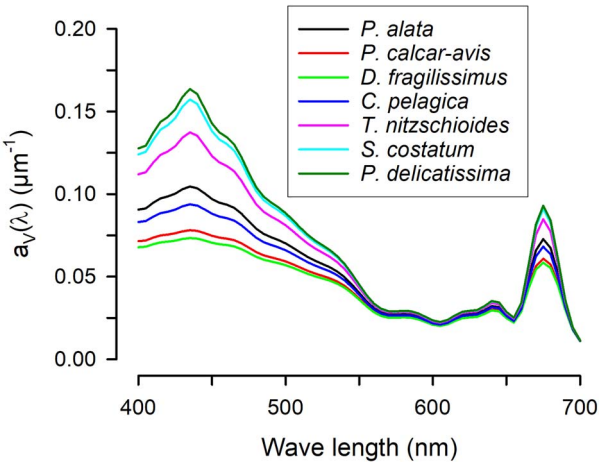

Fig. 5. Spectral dependence of volume-specific light absorption coefficients (by a unit of cell volume) $a_V(\lambda)$ (μm^{-1} = μm^2 × μm^{-3}) for cells of the dominant phytoplankton. The intracellular concentration of chlorophyll a was taken as 4 g L^{-1}.

The dominant and subdominant phytoplankton of the NE of the Black Sea represented a wide range of cell volumes of diatoms; the minimum and maximum biovolumes differed by four orders of magnitude (Table II). The variation in the biovolume of individual chloroplasts did not exceed one order (Table II). The largest individual chloroplasts were seen in the genus *Chaetoceros*; large diatoms had relatively small individual chloroplasts, except the late-autumn dominant *H. hauckii*. The average light path length passing through the chloroplast, $<l>$, was minimal in large diatoms and maximal in representatives of the genus *Chaetoceros* (Table II).

The ability of cells to absorb energy per unit volume of chloroplasts in all the studied algae species did not differ significantly and, on average, was 0.312 ± 0.004 μm^{-1} (μm^{-2}: μm^{-3}) (Table III). The formation of chloroplast aggregates led to a change in the absorbed energy's spectral function, and a flattening effect was observed (Fig. 6). In chloroplast aggregates, the absorbed light energy decreased from 2.5 to 5 times (Table II). *H. hauckii* showed the most significant variability of the volume-specific light absorption coefficient. The summer-dominant diatoms, *P. calcar-avis* and *P. alata*, had approximately the same variability in light absorption due to formation of chloroplast aggregates.

Table III: Volume light absorption coefficient of single chloroplasts and aggregates in the main dominant phytoplankton species. NA, not applicable (no aggregate is formed)

Species	Number of chloroplast in the aggregate	a_V of single chloroplast, μm^{-1}	a_V of the aggregate, (μm^{-1})
Pseudo-nitzschizia pseudodelicatissima	0	0.273	NA
S. costatum	0	0.251	NA
L. danicus	0	0.292	NA
C. affinis	0	0.224	NA
C. curvisetus	0	0.220	NA
C. pelagica	0	0.312	NA
D. fragilissimus	0	0.292	NA
P. alata	50	0.312	0.1212
H. hauckii	100	0.305	0.0615
P. calcar-avis	100	0.316	0.0936

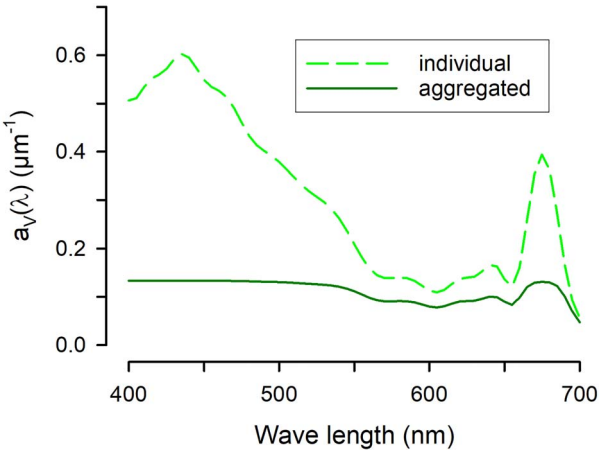

Fig. 6. Spectral dependence of the volume-specific light absorption coefficient (μm^{-1}) per unit volume of an individual chloroplast (bright green) and an aggregate (dark green) of 100 chloroplasts for the centric diatom *P. calcar-avis* with a diameter of 10 μm.

DISCUSSION

The phenomenon of the dominance of large diatoms

Large diatoms are an integral part of the seasonal dynamics of phytoplankton in the Black Sea. In our studies we saw them dominate over periods of several months across two seasons (summer and autumn), in contrast to the short-term spring bloom of small diatoms followed by the somewhat more extended bloom of coccolithophores. The standing stock biomass of large diatoms during the summer intensive growth could be very high, attaining 4 g wet weight m^{-3}. This biomass significantly exceeded that of the dominant small diatoms during the spring blooms and of the coccolithophore bloom in late spring and early summer. Such high biomasses of large diatoms is not exclusively a characteristic feature of the pelagic ecosystem of the Black Sea; it is seen also in ocean waters from the tropics to the northern latitudes (Kemp *et al.*, 2006; Villareal *et al.*, 2012).

The second characteristic feature of the bloom of large diatoms in the Black Sea was the complete dominance of very few species; the contribution to those few diatoms amounted to ca. 99% of the total biomass of eukaryotic phytoplankton. These blooms were almost a monoculture, accompanied usually at a lesser level with a single additional species. This competitive success of large diatoms warrants an explanation. The peculiarity of the pelagic ecosystem of the Black Sea sees this dominance mainly provided by two diatoms—*P. calcar-avis* and *P. alata*. Simultaneously, the first species dominated in mid-summer, the second species usually in early autumn. What is the difference in the ecophysiology of these species that aligns with these regular changes in environmental conditions? Without identifying the conditions of these species' dominance, it is impossible to understand the drivers of the change of dominants that might occur with climate change.

Conditions of dominance

In late May and early June, *Emiliania huxleyi* blooms almost annually in the Black Sea (Pautova *et al.*, 2007; Mikaelyan *et al.*, 2015; Silkin *et al.*, 2019). This period is characterized by a high sharp thermocline and shoaling mixed-layer depth (MLD) (up to a depth of 7 m), a change from complete calm to increased wind, and the highest level of sunlight. There is a change in the wind direction in mid-June, with the NE winds becoming dominant with an additional periodic intensification (Arkhipkin *et al.*, 2014). At this time, there is a change of plankton dominants towards large diatoms. This time is still characterized by high irradiance, and a continuing increase in temperature in the surface water towards the maximum temperature for the entire seasonal cycle. Also, during the summer, the

silicon concentration is significantly decreased, due to the intensive consumption of diatoms. There is a concurrent low phosphorus concentration and a high nitrogen-to-phosphorus inorganic nutrient ratio. For example, during high biomass blooms of *P. calcar-avis*, the following levels of hydrochemical parameters were obtained (Silkin *et al*., 2019), μM: P = 0.03 ± 0.02, N = 1.04 ± 0.9, Si = 1.14 ± 0.37, and N:P = 97 ± 62.

An essential characteristic of the conditions under which large diatoms dominate is that the MLD is constantly deepening over this period, a trend that persists throughout the dominance of these organisms. Thus, typically, the MLD is about 10 m in June, deepening to >25 m by July, and in October, it reaches 40 m. Also, the wind load modulation leads to variability in the deepening of the seasonal thermocline. The consequences of this is that phytoplankton are subjected to significant changes in irradiance; movement in the UML from the surface with a high level of irradiance to the seasonal thermocline depth sees the irradiance fall by two orders of magnitude. The phytoplankton are thus (potentially) moved from the photoinhibition zone to the light-limiting conditions, and back again. To maximize photosynthetic production, while minimizing photoinhibition and photodamage, requires constant adjustment of the photosynthetic apparatus. The light-harvesting pigment complex and the complex photoprotective pigments are always in a mode of continuous acclimation (Falkowski and La Roche, 1991), but especially in these waters, time is crucial for acclimation as it has to occur within ca. an hour (Ross *et al*., 2008; Ross and Geider, 2009). Competitive success will lay with the species that possesses the most cost effective and efficient photoacclimation systems.

Classical ideas about photosynthesis are based on two photochemical stages, which are connected by photosystems I and II. Each photosystem includes a reaction center and antenna pigments. They are enclosed in chloroplasts. During the evolution of photoautotrophic organisms, a large variety in the size, number, morphology, and distribution of chloroplasts has developed (Larkum and Vesk, 2003; Kirk, 2011). Depending on the species and environmental conditions, the number of chloroplasts varies widely from one chloroplast per cell to over a hundred. Small diatoms, which dominant spring blooms as occurs in the Black Sea, have two chloroplasts; in contrast, the large-celled summer dominant *P. calcar-avis* contains more than one hundred chloroplasts. Long-term acclimation to high PFD sees a decrease in chlorophyll concentration in the cell and, above all, a decrease in the number of photosynthetic units (Falkowski and Owens, 1980; Kulk *et al*., 2011). In small diatoms, acclimation to increased PFD is associated primarily with a decrease in the volume of the individual chloroplast. Large diatoms, however, have an additional degree of freedom, namely, to change the number of chloroplasts in the cell and/or their arrangement.

A decrease in the chloroplast volume in small diatoms leads to an increase in the chlorophyll-specific absorption coefficient, thereby part-countering the regulatory effect of a decrease in chlorophyll concentration in the cell (Wilhelm *et al*., 2014). Among the mechanisms of short-term acclimation to high light, small photoautotrophs exploit the formation of xanthophyll cycle pigments to allow them to release excess energy and thereby prevent photoinhibition (Brunet *et al*., 2011; Torres *et al*., 2014). However, this pathway of protection against the pigment apparatus's photodamage does not significantly affect chlorophyll-specific absorption coefficient (Larkum and Vesk, 2003; Raven and Geider, 2003).

The absorption of light by the cell depends on chlorophyll's concentration in the cell and the cell size (Morel and Bricaud, 1981; Finkel, 2001). The ratio of the absorption spectra in solution to that *in vivo* depends on these parameters. However, increasing the cell size allows additional scope for self-shading because the chloroplasts can be packaged, and rearranged, in different ways (Duysens 1956; Key et al., 2011); chloroplasts located closer to the cell wall receive significantly more energy than chloroplasts closer to the center. This phenomenon is the package effect of the first—kind. This package effect decreases the chlorophyll-specific absorption coefficient (Agustı, 1991). Also, as the cell size increases, the value of Chl cell^{-1} decreases (Finkel and Irwin, 2000; Finkel *et al*., 2004). All this inevitably affects the light growth curve parameters, such as the initial slope of the growth-irradiance curve and the maximum specific growth rate. These parameters are interrelated, and an increase in the initial slope of the growth-irradiance curve is accompanied by an increase in the maximum specific growth rate (Edwards *et al*., 2015), depending ultimately on the RuBisCO content (Flynn and Raven, 2017). The initial slope of the growth-irradiance curve reflects light energy use efficiency and is maximal in small cells. In large cells, the initial slope of the growth-irradiance curve is lessened because of the self-shadowing effect, which determines the specific light absorption coefficient (Jones *et al*., 2014).

Chlorophyll is unevenly distributed in large cells, and chloroplasts play the primary role in regulating the cell's optical properties. The size spectrum of chloroplasts is variable, showing interspecific differences. Still, large cells have a relatively small total volume of chloroplasts, which allows them to have a high specific absorption coefficient. Large celled species of diatoms have the capability, the space, to aggregate their chloroplasts, which allows them to change the cell optical properties rapidly over a short time; the specific absorption coefficient significantly

decreases. This effect leads to a significant decrease in the absorbed energy, decreasing the risk of photodamage to the pigment apparatus. This effect is the second—kind of package effect, and it has a significantly shorter response time as it depends on protoplasmic streaming to move chloroplasts around within the cell rather than the synthesis, or dismantling of the photosynthetic machinery. That is why it is singled out as a separate kind of photoacclimation; it differs from the alternative short-term acclimation which is dependent upon the xanthophyll cycle, and is perhaps more efficient. Since dark reactions set limitations on light energy processing (Flynn and Raven, 2017), the excess energy must be discharged as heat, which has consequences for the cell.

The second kind of package effect also provides an additional mechanism for fine-tuning the amount of energy absorbed—this is the functioning of the conveyor to rotate chloroplasts inside the cell, to and from the aggregates (Figs 4 and 6). It can be assumed that with a low *in situ* PFD, such as at the depth of the seasonal thermocline, the chloroplasts are distributed evenly throughout the cell volume. When the cells are moved upward, into shallower depths with increasing PFD, the formation of the chloroplast aggregates begins, and the conveyor starts. The duration of the conveyor cycle is regulated by the irradiance, decreasing with increasing PFD as more chloroplasts are held centrally in aggregates. In cells at the water's surface, with maximum irradiance, we expect the conveyor to stop, the chloroplasts having been moved from wall to the cell center in aggregates. We hypothesize that the dose of absorbed energy is the controlling factor for the rate of this chloroplast movement. Collectively these events control the dose of absorbed energy to individual chloroplasts, modulating the dose to the whole organism. The mechanism thus mitigates against the risk of individual chloroplast exceeding the critical photon dose, minimizing the potential consequential permanent photodamage.

The decrease in the specific absorption coefficient per unit volume of chloroplasts in the aggregates is decreased by at least three times (Fig. 6). In other words, at a maximum PFD for wavelengths from 400 to 700 nm, of about 1000 μmol m^{-2} s^{-1}, such irradiation at the water surface is perceived by chloroplasts arranged in aggregates as only 200–400 μmol quanta m^{-2} s^{-1}. This perceived irradiance level is in the region of photon saturation, rather than photoinhibition, for many species (Bouman *et al*., 2018). When the cells are moved to deeper waters, the process is reversed. We found such a fine-tuning mechanism of the absorbed energy in two large-cell species—*P. calcar-avis* and *H. hauckii*. The latter species periodically dominate at the end of the autumn with it growing in an enormously deepened thermocline when the irradiance gradient between the surface water and the thermocline is at its extreme. *H. hauckii* has a low speed of movement of chloroplasts and, at the same time, a shorter conveyor length (shorter cell form).

The second kind of packing allows large cells to retain a high chlorophyll concentration without the attendant risks of photodamage because they can rapidly change (adjust) the specific absorption coefficient. Ultimately, this contributes to an increase in the growth rate of the cell in low-light conditions. Considering the content of chlorophyll in the cell in the context of two opposite processes (photodamage and repair of chlorophyll molecules), it should be noted that the repair of photosystems requires significant energy costs as well as *de facto* taking the carbon fixation system off-line (it is no longer functioning efficiently), all of which decreases cell growth (Raven, 2011). Also, there are non-energy costs for the synthesis of chlorophyll, and here, the main factor may be the availability of nutrients. The synthesis of chlorophyll and the allied photosystem structure involves the assimilation of nitrogen (Geider *et al*., 1998, 2009). It has also been shown that photosystem II activity in small diatoms is susceptible to nitrogen deficiency (Loebl *et al*., 2010). Indeed, a short-term increase in the nitrogen concentration in surface water returns the small diatom *P. pseudodelicatissima* to dominance in the Black Sea; we observed this phenomenon several times in August when a strong NE wind caused upwelling, which significantly increased inorganic nitrogen concentration in the water. Large diatoms, such as *P. calcar-avis*, have the potential to accumulate nutrients due to a large proportion of vacuoles in the cell volume (Dortch *et al*. 1984; Raven, 1987); such a resource provides readily available nutrient (in the form of free amino acids) for repair processes. Such scope would be lessened in small diatoms which also have a higher biomass density as well as a lower vacuole volume. Another key factor is the recovery time of the light-harvesting complex after photodamage (Raven, 2011), which can be significantly higher than the short-term photoacclimation of the second kind.

We hypothesize that the location for repair of chloroplasts are within the aggregates where they are protected from the damaging effects of light. Set in the context of a cost–benefit analysis (Geider *et al*., 2009; Raven, 2011), the costs of synthesis and maintenance of the chloroplast movement systems in large diatoms appear readily justified from the point of view of providing a competitive advantage. They ensure these diatoms' evolutionary fitness in conditions of highly fluctuating PFD and low nutrient concentrations. They allow the preservation of the photosystem complex in a favorable state in unfavorable environmental conditions, and then enable them to optimize the use of light energy as that

energy changes. It is likely that these large diatoms persist in low nutrient ecosystems, with a maximum specific growth rate evolved to maximize growth potential while minimizing stress (Flynn and Skibiniski, 2020), exploiting what pulses of nutrients come their way. The accumulative hypothesis for the dominance of large diatoms (Tozzi *et al*., 2004; Verdy *et al*., 2011; Silkin *et al*., 2019) is thus part-and-parcel of the photoacclimation hypothesis we explore here. Large diatoms are able to accumulate the nutrients with the periodic intensification of vertical exchange and consume them in a stable environment with a low nutrient concentration. These species are storage machineries, with nitrogen-to-phosphorus ratios in the cell significantly higher than the Redfield ratio (Klausmeier *et al*., 2004), low growth rates (consistent with the growth rate hypothesis; Rees and Raven, 2021). Mathematical modeling of population dynamics, suggests that these species can become dominant in conditions with a periodic regime of providing of the nutrients (Stolte and Riegman, 1996; Litchman *et al*., 2009; Abakumov *et al*., 2011). This hypothesis alone may not explain the dominance of large diatoms because the effect of nutrients storage affects only at the level of one-two generation (Behrenfeld *et al*., 2021a). However, as an integral part of our hypothesis, it can still provide a resource potential for repair processes in the chloroplast. The critical issue, though, is the ability of large diatoms to optimize the photoenergetic supply of the cell in a dynamic environment. It is also notable that in models of phytoplankton photoacclimation, the rate of acclimation and not just the end points is an important feature of the model (Flynn *et al*., 2001).

The persistence of large diatom blooms critically also requires low loss rates. Large diatoms cells are eaten only by large zooplankton due to their size characteristics (Kiørboe, 2011; Ward *et al*., 2012). The dominance of large diatoms under high light conditions can be explained by selective grazing of small phytoplankton by microzooplankton. The prevalence of small size phytoplankton in low-light conditions is controlled by mesozooplankton (Wirtz, Sommer, 2013). However, in the Black Sea the predatory factor appears secondary to the nutrients and energy supply of growth; predation can play a role in accelerating the removal of small diatoms from the community, but alone it cannot be the driving factor of selective shift. The existence of a time lag before the appearance of a predator for large diatoms may contribute to more intensive biomass growth at the initial stages of the bloom development. The highest abundance of zooplankton in NE Black Sea is observed in August and September, but at this time large diatoms are already growing intensively.

CONCLUSION

The rapid-response photoacclimation system we report, combined with a storage strategy for nutrients, creates in Black Sea large diatoms a unique biological machine well adapted to the dynamic environment. Active growth can be maintained in a highly gradient light and nutrient environment, leaving other species with little chance to compete. Grazing losses are low (as these diatoms bloom at a time of high zooplankton abundance), and the risks of virus attack on such large cells will likely be similarly low (Flynn *et al*., 2021). The populations collapse at the end of the season when physical forces change the UML, and reintroduce nutrients to support the success of other species growing in the decreasing sunlight of autumn. As for the new mandala for diatom success (Behrenfeld *et al*. 2021b), our photo-energetic concept complements it with another energetic coordinate and shows that the evolution towards large diatoms was due to a new vector—the ability of cells to change the absorbed energy of light by changing the specific absorption coefficient, not changing the cell concentration of chlorophyll.

SUPPLEMENTARY DATA

Supplementary data can be found at *Journal of Plankton Research* online.

AUTHOR'S CONTRIBUTIONS

V. Silkin conducted calculations of the absorption coefficients and wrote the paper. A. Fedorov conducted laboratory experiments. K.J. Flynn contributed to interpretation and writing of the paper. L. Paramonov developed a theoretical approach. L. Pautova provided the field data.

COMPETING INTERESTS

We have no competing interests.

DATA ACCESSIBILITY

Data will be published in Data in Brief.

FUNDING

Ministry of Science and Higher Education of the Russian Federation (theme no. 0128-2021-0013). Russian Science Foundation grant (project no. 20-17-00167) and the Russian Foundation for Basic Research (project no. 19-05-50090).

REFERENCES

Abakumov, A. I., Silkin, V. A. and Pautova, L. A. (2011) Biomass dynamics of the phytoplankton under impact of the nutrient. *Proc. Environ. Sci.*, **8**, 105–110.

Agusti, S. (1991) Allometric scaling of light absorption and scattering by phytoplankton cells. *Can. J. Fish. Aquat. Sci.*, **48**, 763–767.

Armbrust, E. V. (2009) The life of diatoms in the world's oceans. *Nature*, **459**, 185–192.

Arkhipkin, V. S., Gippius, F. N., Koltermann, K. P. and Surkova, G. V. (2014) Wind waves in the Black Sea: results of a hind cast study. *Nat. Hazards Earth Syst. Sci.*, **14**, 2883–2897. 10.5194/nhess-14-2883-2014.

Barton, A. D., Ward, B. A., Williams, R. G. and Follows, M. J. (2014) The impact of fine-scale turbulence on phytoplankton community structure. *Limnol. Oceanogr: Fluid. Environ.*, **4**, 34–49. 10.1215/21573689-2651533.

Behrenfeld, M. J., Halsey, K. H., Boss, E., Karp-Boss, L., Milligan, A. J. and Peers, G. (2021a) Thoughts on the evolution and ecological niche of diatoms. *Ecol. Monogra.*, **91**, e01457. 10.1002/ecm.1457.

Behrenfeld, M. J., Boss, E. and Halsey, K. H. (2021b) Phytoplankton community structuring and succession in a competition-neutral resource landscape. *ISME Commun.*, **1**, 12. 10.1038/S43705-021-00011-5.

Bouman, H. A., Platt, T., Doblin, M., Figueiras, F. G., Gudmundsson, K., Gudfinnsson, H. G., Huang, B., Hickman, A. *et al.* (2018) Photosynthesis–irradiance parameters of marine phytoplankton: synthesis of a global data set. *Earth Syst. Sci. Data*, **10**, 251–266.

Blatt, M. R., Weisenseel, M. H. and Haupt, W. (1981) A light-dependent current associated with chloroplast aggregation in the alga *Vaucheria sessilis*. *Planta*, **152**, 513–526. 10.1007/BF00380822.

Bordovskiy, O. K. and Chernyakova, A. M. (eds.) (1992) *Modern methods of the ocean hydrochemical investigations. P.P*, Shirshov Institute of Oceanology, Moscow, 200 p. (in Russian).

Brunet, C., Johnsen, G., Lavaud, J., and Roy, S. (2011) Pigments and photoacclimation processes. In Roy, S., Llewellyn, C. A., Egeland, E. S. and Johnsen, G.(eds), *Phytoplankton Pigments*; Cambridge Press University, UK. doi:10.1017/CBO9780511732263.017

Chen, S. T. and Li, C. W. (1991) Relationships between the movements of chloroplasts and cytoskeletons in diatoms. *Botanica Marina*, **34**, 505–511. 10.1515/botm.1991.34.6.505.

Chisholm, S. W. (1992) *Phytoplankton size*. In Falkowski, P. G., Woodhead, A. D., Vivirito, K. (eds) *Primary Productivity and Biogeochemical Cycles in the Sea. Environ. Sci. Res*, **43** Springer, Boston, MA. doi:10.1007/978-1-4899-0762-2_12

Droop, M. R., Mickelson, M. J., Scott, J. M. and Turner, M. F. (1982) Light and nutrient status of algal cells. *J. Mar. biol. Assoc. U.K.*, **62**, 403–434.

Duysens, L. N. M. (1956) The flattening of the absorption spectra of suspensions as compared to that of solutions. *Biochim. Biophys. Acta*, **19**, 1–12. 10.1016/0006-3002(56)90380-8.

Edwards, K. F., Thomas, M. K., Christopher, A., Klausmeier, A. C. and Litchman, E. (2012) Allometric scaling and taxonomic variation in nutrient utilization traits and maximum growth rate of phytoplankton. *Limnol. Oceanogr.*, **57**, 554–566. 10.4319/lo.2012.57.2.0554.

Edwards, K. F., Thomas, M. K., Christopher, A., Klausmeier, A. C. and Litchman, E. (2015) Light and growth in marine phytoplankton: allometric, taxonomic, and environmental variation. *Limnol. Oceanogr.*, **60**, 540–552. 10.1002/lno.10033.

Falkowski, P. G. and Owens, T. G. (1980) Light–shade adaptation: two strategies in marine phytoplankton. *Plant Physiol.*, **66**, 592–595. 10.1104/pp.66.4.592.

Falkowski, P. G. and LaRoche, J. (1991) Acclimation to spectral irradiance in algae. *J Phycol.*, **27**, 8–14.

Finkel, Z. V. (2001) Light absorption and size scaling of light-limited metabolism in marine diatoms. *Limnol. Oceanogr.*, **46**, 86–94.

Finkel, Z. V. and Irwin, A. J. (2000) Modeling size-dependent photo synthesis: light absorption and the allometric rule. *J. Theor. Biol.*, **204**, 361–369.

Finkel, Z. V., Irwin, A. J. and Schofield, O. (2004) Resource limitation alters the $^3/_4$ size scaling of metabolic rates in phytoplankton. *Mar. Ecol. Prog. Ser.*, **273**, 269–279.

Flynn, K. J. and Raven, J. A. (2017) What is the limit for photoautotrophic plankton growth rates? *J. Plankton Res.*, **39**, 13–22. 10.1093/plankt/fbw067.

Flynn, K. J. and Skibinski, D. O. F. (2020) Exploring evolution of maximum growth rates in plankton. *J. Plankton Res.*, **42**, 497–513. 10.1093/plankt/fbaa038.

Flynn, K. J., Marshall, H. and Geider, R. J. (2001) A comparison of two N-irradiance models of phytoplankton growth. *Limnol. Oceanogr.*, **46**, 1794–1802.

Flynn, K. J., Skibinski, D. O. F. and Lindemann, C. (2018) Effects of growth rate, cell size, motion, and elemental stoichiometry on nutrient transport kinetics. *PLoS Comput. Biol.*, **14**, e1006118. 10.1371/journal.pcbi.1006118.

Flynn, K. J., Kimmance, S. A., Clark, D. R., Mitra, A., Polimene, L. and Wilson, W. H. (2021) Modelling the effects of traits and abiotic factors on viral lysis in phytoplankton. *Front. Mar. Sci.*, **8**, 667184. 10.3389/fmars.2021.667184.

Furukawa, T., Watanabe, M. and Shihira-Ishikawa, I. (1998) Green- and bluelight-mediated chloroplast migration in the centric diatom *Pleurosira laevis*. *Protoplasma*, **203**, 214–220. 10.1007/BF01279479.

Geider, R. J., MacIntyre, H. L. and Kana, T. M. (1998) A dynamic regulatory model of phytoplankton acclimation to light, nutrients and temperature. *Limnol. Oceanogr.*, **43**, 679–694.

Geider, R. J., Moore, C. M. and Ross, O. N. (2009) The role of cost–benefit analysis in models of phytoplankton growth and acclimation. *Plant Eco. Div.*, **2**, 165–178. 10.1080/17550870903300949.

Gemmell, B. J., Oh, G., Buskey, E. J. and Villareal, T. A. (2016) Dynamic sinking behaviour in marine phytoplankton: rapid changes in buoyancy may aid in nutrient uptake. *Proc. R. Soc. B*, **283**, 20161126. 10.1098/rspb.2016.112.

Goessling, J. W., Cartaxana, P. and Kühl, M. (2016) Photo-protection in the centric diatom *Coscinodiscus granii* is not controlled by chloroplast high-light avoidance movement. *Front. Mar. Sci.*, **2**, 115. 10.3389/fmars.2015.00115.

Goldman, J. C. (1993) Potential role of large oceanic diatoms in new primary production. *Deep Sea Res. Part I: Oceanogr. Res. Pap.*, **40**, 159–168. 10.1016/0967-0637(93)90059-C.

Grashoff, K., Kremling, K. and Ehrhard, M. (1999) *Methods of Seawater Analysis*, Wiley-VCH, Weinheim-New York-Chichester-Brisbane-Singapore-Toronto, p. 420.

Grover, J. P. (1989) Influence of cell shape and size on algal competitive ability. *J. Phycol.*, **25**, 402–405.

Grover J.P. (1997) Resource competition and evolution. In *Resource Competition. Pop. Comm. Biol. Ser.*, **19**. Springer, Boston, MA. doi:10.1007/978-1-4615-6397-6_9

Hamm, C. E., Merkel, R., Springer, O., Jurkojc, P., Maier, C., Prechtel, K. and Smetacek, V. (2003) Architecture and material properties of

diatom shells provide effective mechanical protection. *Nature*, **421**, 841–843.

Hillebrand, H., Durselen, C., Kirschtel, D., Pollingher, U. and Zohary, T. (1999) Biovolume calculation for pelagic and benthic microalgae. *J. Phycol.*, **35**, 403–424.

Hoepffner, N. and Sathyendranath, S. (1991) Effect of pigment composition on absorption properties of phytoplankton. *Mar. Ecol. Prog. Ser.*, **73**, 11–23.

Huisman, J., Pham Thi, N. N., Karl, D. M. and Sommeijer, B. (2006) Reduced mixing generates oscillations and chaos in the oceanic deep chlorophyll maximum. *Nature*, **439**, 322–325.

Jenkin, P. M. (1937) Oxygen production by the diatom *Coscinodiscus excentricus* Ehr. In relation to submarine irradiance in the English Channel. *J. Mar. Biol. Assoc. UK*, **22**, 301–342.

Jones, C. T., Craig, S. E., Barnett, A. B., MacIntyre, H. L. and Cullen, J. J. (2014) Curvature in models of the photosynthesis-irradiance response. *J. Phycol.*, **50**, 341–355. 10.1111/jpy.12164.

Kemp, A., Pearce, R. B., Grigorov, I., Rance, J., Lange, C. B., Quilty, P. and Salteet, I. (2006) Production of giant marine diatoms and their export at oceanic frontal zones: implications for Si and C flux from stratified oceans. *Global Biogeochem Cycles*, **20**, 1–3.

Key, T., McCarthy, A., Campbell, D. A., Six, C., Roy, S. and Finkel, Z. V. (2010) Cell size trade-offs govern light exploitation strategies in marine phytoplankton. *Env. Microbiol.*, **12**, 95–104. 10.1111/j.1462-2920.2009.02046.x.

Kiefer, D. (1973) Chlorophyll a fluorescence in marine centric diatoms: responses of chloroplasts to light and nutrient stress. *Mar. Biol.*, **23**, 39–46. 10.1007/BF00394110.

Kiefer, D. A. and Mitchell, B. G. (1983) A simple, steady state description of phytoplankton growth rates based on absorption cross section and quantum efficiency. *Limnol. Oceanogr.*, **28**, 770–776.

Kiørboe, T. (2008) *A Mechanistic Approach to Plankton Ecology*, Princeton University Press, USA, 224 p.

Kiørboe, T. (2011) How zooplankton feed: mechanisms, traits and trade-offs. *Biol. Rev. Cam. Phil. Soc.*, **86**, 311–339.

Kirk, J. T. O. (2011) *Light and Photosynthesis in Aquatic Ecosystems*, 3rd edn, Cambridge University Press, New York, p. 649.

Klausmeier, C. A., Litchman, E., Daufresne, T. and Levin, S. A. (2004) Optimal nitrogen-to-phosphorus stoichiometry of phytoplankton. *Nature*, **429**, 171–174. 10.1038/nature02454.

Kulk, G., VAN DE Poll, W. H., Visser, R. J. W. and Buma, A. G. J. (2011) Distinct differences in photoacclimation potential between prokaryotic and eukaryotic oceanic phytoplankton. *J. Exp. Mar. Biol. Ecol.*, **398**, 63–72. 10.1016/j.jembe.2010.12.011.

Larkum, A. W., and Vesk, M. (2003) Algal plastids: Their fine structure and properties. In A. W. Larkum, S. E. Douglas, & J. A. Raven (eds). *Photosynthesis in Algae*. Kluwer Academic Publ, Dordrecht, The Netherlands, pp. 11–28. doi:10.1007/978-94-007-1038-2_2

Laws, E. A., Falkowski, P. G., Smith, W. O. J., Ducklow, H. and McCarthy, J. J. (2000) Temperature effects on export production in the open ocean. *Global Biogeochem. Cycles*, **14**, 1231–1246.

Litchman, E. and Klausmeier, C. A. (2001) Competition of phytoplankton under fluctuating light. *Amer. Nat.*, **157**, 170–187. 10.1086/318628.

Loebl, M., Cockshutt, A. M., Campbell, D. A. and Finkel, Z. V. (2010) Physiological basis for high resistance to photoinhibition under nitrogen depletion in *Emiliania huxleyi*. *Limnol. Oceanogr.*, **55**, 2150–2160. 10.4319/lo.2010.55.5.2150.

MacIntyre, H. L., Kana, T. M., Anning, J. and Geider, R. (2002) Photoacclimation of photosynthesis irradiance response curves and photosynthetic pigments in microalgae and cyanobacteria. *J. Phycol.*, **38**, 17–38.

Margalef, R. (1978) Life forms of phytoplankton as survival alternatives in an unstable environment. *Oceanol. Acta*, **1**, 493–509.

McBeain, K. H. and Halsey, K. A. (2018) Altering phytoplankton growt rates changes their value as food for microzooplankton grazers. *Aquat. Microbial Ecol.*, **82**, 19–29. 10.3354.ame01880.

Menden-Deuer, S. and Lessard, E. J. (2000) Carbon to volume relationships for dinoflagellates, diatoms, and of the protist plankton. *Limnol. Oceanogr.*, **45**, 569–579.

Mikaelyan, A. S., Pautova, L. A., Chasovnikov, V. K., Mosharov, S. A. and Silkin, V. A. (2015) Alternation of diatoms and coccolithophores in the northeastern Black Sea: a response to nutrient changes. *Hydrobiologia*, **755**, 89–105. 10.1007/s10750-015-2219-z.

Morel, A. and Bricaud, A. (1981) Theoretical results concerning light absorption in a discrete medium, and application to specific absorption of phytoplankton. *Deep Sea Res.*, **28**, 1375–1393. 10.1016/0198-0149(81)90039-X.

Nobel, P. S. (2005) *Physicochemical and Environmental Plant Physiology*, 3rd edn, Academic Press/Elsevier, p. 540.

Paramonov, L. E. (2018) The spectrum of absorption indices and the intracellular concentration of pigments of cyanobacteria by the example of *Spirulina platensis*. *Optics Atmos. Ocean*, **31**, 103–108.

Pautova, L. A., Mikaelyan, A. S. and Silkin, V. A. (2007) The structure of plankton community in shelf waters of north-eastern part of the Black Sea in the period of mass bloom of *Emiliania huxleyi* in 2002-2005. *Oceanology*, **47**, 408–417.

Raven, J. A. (1987) The role of vacuoles. *New Phytol.*, **106**, 357–422.

Raven, J. A. (2011) The cost of photoinhibition. *Physiol. Plant.*, **142**, 87–104. 10.1111/j.1399-3054.2011.01465.x.

Raven, J. A. and Geider, R. J. (2003) Adaptation, acclimation and regulation in algal photosynthesis. In Larkum, A. W. D., Douglas, S. and Raven, J. A. (eds.), *Photosynthesis of Algae*, Kluwer Academic, Dordrecht, the Netherlands, pp. 385–412.

Rees, T. A. V. and Raven, J. A. (2021) The maximum growth rate hypothesis is correct for eukaryotic photosynthetic organisms, but not cyanobacteria. *New Phytol.*, **230**, 601–611. 10.1111/nph.17190.

Richardson, K., Beardall, J. and Raven, J. A. (1983) Adaptation of unicellular algae to irradiance: an analysis of strategies. *New Phytol.*, **93**, 157–191.

Richardson, T. L., Ciotti, A. M., Cullen, J. J. and Villareal, T. A. (1996) Physiological and optical properties of *Rhizosolenia formosa* (Bacillariophyceae) in the context of open-ocean vertical migration. *J. Phycol.*, **32**, 741–757.

Ross, O. N., Moore, M. C., Suggett, D. J., MacIntyre, H. L. and Geider, R. J. (2008) A model of photosynthesis and photo-protection based on reaction center damage and repair. *Limnol. Oceanogr.*, **53**, 1835–1852. 10.2307/40058301.

Ross, O. N. and Geider, R. J. (2009) New cell-based model of photosynthesis and photo-acclimation: accumulation and mobilization of energy reserves in phytoplankton. *Mar. Ecol. Prog. Ser.*, **383**, 53–71. 10.3354/meps07961.

Silkin, V. A., Pautova, L. A., Giordano, M., Chasovnikov, V. K., Vostokov, S. V., Podymov, O. I., Pakhomova, S. V. and Moskalenko, L. V. (2019) Drivers of phytoplankton blooms in

the northeastern Black Sea. *Mar. Poll. Bull.*, **138**, 274–284. 10.1016/j.marpolbul.2018.11.042.

Smetacek, V. (1999) Diatoms and the ocean carbon cycle. *Protist*, **150**, 25–32. 10.1016/S1434-4610(99)70006-4.

Stolte, W. and Riegman, R. (1996) A model approach for size-selective competition of marine phytoplankton for fluctuating nitrate and ammonium. *J Phycol.*, **32**, 732–740.

Suggett, D. J., Le Floch, E., Harris, G. N., Leonardos, N. and Geider, R. J. (2007) Different strategies of photoacclimation by two strains of *Emiliania huxleyi* (Haptophyta). *J. Phycol.*, **43**, 1209–1222. 10.1111/j.1529-8817.2007.00406.x.

Sydko, F. Y., Belyanin, V. N., Gevel, L. M. and Eroshin, N. S. (1966) To the mathematical theory of photosynthesis of microalgae culture. In Terskov, I. A. (ed.), *Controllable Biosynthesis*, Science, Moscow, pp. 32–39.

Torres, M. A., Ritchie, R. J., McC-Lilley, R., Grillet, C. and Larkum, A. W. D. (2014) Measurement of photosynthesis and photosynthetic efficiency in two diatoms. *New Zea. J. Bot.*, **52**, 6–27. 10.1080/0028825X.2013.831917.

Treguer, P. J. and De La Rocha, C. L. (2013) The world ocean silica cycle. *Ann. Rev. Mar. Sci.*, **5**, 477–501. 10.1146/annurev–marine-121211-172346.

Tomas, C. R. (1997) *Identifying Marine Phytoplankton*, Academic Press, San Diego, US ISBN 0-12-693018-X. XV, p. 858.

Tozzi, S., Schofield, O. and Falkowski, P. (2004) Historical climate change and ocean turbulence as selective agents for two key phytoplankton functional groups. *Mar. Ecol. Prog. Ser.*, **274**, 123–132. 10.3354/meps274123.

Throndsen, J., Hasle, G. R. and Tangen, K. (2003) *Norsk kystplanktonflora*, Almater Forlag AS, Oslo, p. 341.

Verdy, A., Follows, M. and Flierl, G. (2009) Optimal phytoplankton cell size in an allometric model. *Mar. Ecol. Prog. Ser.*, **379**, 1–12. 10.3354/meps07909.

Villamaña, M., Marañón, E., Cermeño, P., Estrada, M., Fernández-Castro, B., Figueiras, F. G., Latasa, M., Luis Otero-Ferrer, J. *et al.* (2019) The role of mixing in controlling resource availability and phytoplankton community composition. *Prog. Oceanogr.*, **178**, 102181. 10.1016/j.pocean.2019.102181.

Villareal, T. A., Brown, C. G., Brzezinski, M. A., Krause, J. W. and Wilson, C. (2012) Summer diatom blooms in the North Pacific subtropical gyre: 2008–2009. *PLoS One*, **7**, e33109. 10.1371/journal.pone.0033109.

Villareal, T. A., Woods, S., Moore, J. K. and Culver-Rymsza, K. (1996) Vertical migration of *Rhizosolenia* mats and their significance to NO_3^--fluxes in the central North Pacific gyre. *J. Plankton Res.*, **18**, 1103–1121.

Ward, B. A., Dutkiewicz, S., Jahn, O. and Follows, M. J. (2012) A size-structured food-web model for the global ocean. *Limnol. Oceanogr.*, **57**, 1877–1891. 10.4319/lo.2012.57.6.1877.

Wilhelm, C., Jungandreas, A., Jakob, T. and Goss, R. (2014) Light acclimation in diatoms: from phenomenology to mechanisms. *Mar. Genomics*, **16**, 5–15. 10.1016/j.margen.2013.12.003.

Wirtz, K. W. (2012) Who is eating whom? Morphology and feeding type determine the size relation between planktonic predators and their ideal prey. *Mar Ecol Prog Ser.*, **445**, 1–12. 10.3354/meps09502.

Wirtz, K. W. and Sommer, U. (2013) Mechanistic origins of variability in phytoplankton dynamics. Part II: analysis of mesocosm blooms under climate change scenarios. *Mar. Biol.*, **160**, 2503–2516. 10.1007/s00227-013-2271.